Josephson current via an isolated Majorana zero mode

Chun-Xiao Liu [1,*] Bernard van Heck [2] and Michael Wimmer [1]

[1]*Qutech and Kavli Institute of Nanoscience, Delft University of Technology, 2600 GA Delft, Netherlands*
[2]*Microsoft Quantum Lab Delft, Delft University of Technology, 2600 GA Delft, Netherlands*

We study the equilibrium dc Josephson current in a junction between an *s*-wave and a topological superconductor. Cooper pairs from the *s*-wave superconducting lead can transfer to the topological side either via an unpaired Majorana zero mode localized near the junction or via the above-gap continuum states. We find that the Majorana contribution to the supercurrent can be switched on when time-reversal symmetry in the conventional lead is broken, e.g., by an externally applied magnetic field inducing a Zeeman splitting. Moreover, if the magnetic field has a component in the direction of the effective spin-orbit field, there will be a Majorana-induced anomalous supercurrent at zero phase difference. These behaviors may serve as a signature characteristic of Majorana zero modes and are accessible to devices with only superconducting contacts.

I. INTRODUCTION

Majorana zero modes (MZMs) are neutral midgap excitations localized at the defects or wire ends of a topological superconductor [1–12]. Due to their robustness against local perturbations and their non-Abelian statistics, MZMs are potential building blocks for topological quantum computation [13,14]. One of the promising candidates for realizing topological superconductivity in solid-state physics is heterostructures consisting of a one-dimensional Rashba spin-orbit-coupled semiconductor nanowire and a proximitizing conventional *s*-wave superconductor [15–18]. The application of a large enough Zeeman field parallel to the nanowire can drive the hybrid system into the topological superconducting phase, with MZMs forming at the wire ends.

So far, most evidence for MZMs comes from tunneling spectroscopy in normal-metal-superconductor junctions, in which a MZM gives rise to a zero-bias conductance peak [19–29]. In addition, several proposals have been put forward to probe topological superconductivity with superconducting contacts. One advantage of a superconducting lead is that quasiparticle poisoning can be mitigated at temperatures smaller than the gap Δ_0, which is beneficial for qubit proposals [30]. In a voltage-biased junction between trivial and topological superconductors, the MZM will manifest itself as a conductance peak of height $(4 - \pi)2e^2/h$ at $eV = \pm\Delta_0$ in the tunneling limit [31–34]. Several works have considered the equilibrium dc Josephson current between trivial and topological superconductors (see Fig. 1) and have established that the Majorana contribution to the supercurrent is negligible [35–38]. Corrections arise due to the above-gap quasiparticle contributions if the nanowire length is short or if a quantum dot is present between the two leads [38–41].

Existing studies have focused on the case in which time-reversal symmetry (TRS) is present in the trivial superconductor. In practice, however, a magnetic field has to be applied globally to a device, and thus, TRS inside the trivial lead is inevitably broken. In this work, we explore in detail the consequences of TRS breaking in the trivial lead for the Josephson current. We show that a finite Zeeman splitting inside the trivial superconductor generates a Majorana-induced supercurrent. Additionally, if the magnetic field has a component in the direction of the effective spin-orbit field, the MZM induces an anomalous supercurrent, flowing at zero phase difference between the leads. Thus, under appropriate conditions the dc Josephson current in a trivial-topological superconductor junction can provide observable evidence for MZMs.

II. MODEL AND METHOD

The Hamiltonian for the one-dimensional nanowire Josephson junction represented in Fig. 1 is

$$H = H_L + H_R + H_{\text{tunnel}}, \tag{1}$$

where H_L (H_R) is the Hamiltonian for the left (right) nanowire lead [16,17]:

$$H_j = \int dx\, c^{\dagger}_{j\sigma}(x)\,[h_j]_{\sigma\sigma'}\,c_{j\sigma'}(x) + \Delta_0[c_{j\downarrow}(x)c_{j\uparrow}(x) + \text{H.c.}],$$

$$h_j = -\frac{\hbar^2}{2m^*}\partial_x^2 - \mu_j - i\alpha_j\partial_x\sigma_y + \vec{E}_{Z,j}\cdot\vec{\sigma}. \tag{2}$$

Here $j = L, R$, $c^{\dagger}_{j\sigma}(x)$ creates an electron of spin σ in lead j at position x, $\sigma_{x,y,z}$ are the Pauli matrices acting on the spin space, m^* is the effective mass, μ_j is the chemical potential, α_j is the strength of Rashba spin-orbit coupling with the corresponding spin-orbit field pointing along the σ_y direction, Δ_0 is the proximity-induced superconducting gap, and $\vec{E}_{Z,j} = \frac{1}{2}g\mu_B\vec{B}_j$ is the Zeeman field due to the applied
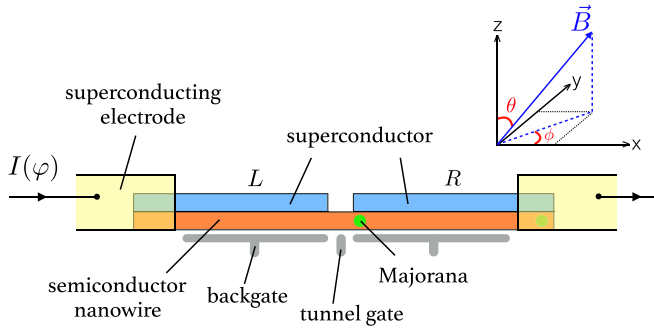
*chunxiaoliu62@gmail.com

FIG. 1. Side-view schematic of a Josephson junction between trivial and topological superconductors. A semiconducting nanowire (orange) is in proximity to two conventional s-wave superconductors (blue) separated by the tunnel junction. An unpaired Majorana zero mode (green dot) can appear near the junction when the right hybrid nanowire becomes topological. The chemical potential of the superconductor can be tuned by the back gate (gray line), while the junction transparency can be controlled by the tunnel gate (gray dot). The inset indicates the coordinate axes and direction of magnetic field.

magnetic field. We have defined parameters separately for the left and right leads, which will allow us to consider different physical scenarios in what follows. We will always assume that the chemical potential in the left lead is set to a high value $\mu_L \gg \Delta_0$, such that the left lead is in the topologically trivial regime. For numerical results, the continuum Hamiltonian in Eq. (2) needs to be discretized into a tight-binding model [42,43]. When doing so, we always take the size L of the left and right leads to be large enough that finite-size effects (e.g., Majorana overlap) play no essential role.

The tunnel Hamiltonian is given by

$$H_{\text{tunnel}} = -t e^{i\varphi/2} \sum_{\sigma=\uparrow\downarrow} c^\dagger_{R\sigma}(x_R) c_{L\sigma}(x_L) + \text{H.c.} \quad (3)$$

and describes spin-conserving single-electron tunneling occurring at a point contact connecting the left lead (ending at $x = x_L$) to the right lead (beginning at $x = x_R$). Here φ is the phase difference between the leads, and t is the tunneling strength, which is associated with the normal conductance by $G_N = 4\pi e^2 t^2 \nu_L \nu_R/\hbar$, with $\nu_{L,R}$ being the normal density of states at the Fermi surface of the left and right leads.

In the tunneling limit $t \ll \Delta_0$, which can always be reached by tuning the tunnel gate, second-order perturbation theory yields the zero-temperature current-phase relation of the junction [44,45],

$$I(\varphi) = I_c \sin(\varphi + \varphi_0). \quad (4)$$

The critical current $I_c = 4et^2|\mathcal{A}|/\hbar$ and the phase shift $\varphi_0 = \arg(\mathcal{A})$ are determined by the amplitude $\mathcal{A}$ of Cooper pair transfer from left to right. The latter is a sum over all possible intermediate states with a quasiparticle in each lead,

$$\mathcal{A} = \sum_{\substack{nm \\ \eta\sigma=\uparrow\downarrow}} \frac{u^*_{Ln\eta}(x_L) v_{Ln\sigma}(x_L) u_{Rm\sigma}(x_R) v^*_{Rm\eta}(x_R)}{E_{Ln} + E_{Rm}}. \quad (5)$$

Here $E_{jn} \geqslant 0$ is the energy of the nth Bogoliubov quasiparticle excitation in lead j, with the Nambu wave function $[u_{jn\uparrow}(x), u_{jn\downarrow}(x), v_{jn\uparrow}(x), v_{jn\downarrow}(x)]^\intercal$. When the right lead is in the topological phase, we can separate the amplitude into two parts, $\mathcal{A} = \mathcal{A}^M + \mathcal{A}^{\text{cont}}$, depending on whether the intermediate state involves an isolated MZM ($E_{Rm} = 0$) or an excited quasiparticle state in the continuum ($E_{Rm} > 0$). At zero field, Eq. (5) yields the classical Ambegaokar-Baratoff relation $I_{c0} = (\pi/2e)G_N \Delta_0$ [44]. When $\varphi_0 \neq 0$ or π, an anomalous supercurrent $I_{\text{an}} = I_c \sin(\varphi_0)$ flows at $\varphi = 0$.

III. MAJORANA-INDUCED SUPERCURRENT

We now focus on a physical scenario that illustrates the joint role of the MZM and TRS breaking in the left lead in generating a supercurrent. Namely, we consider the case in which the parameters of H_R are fixed in the topological regime; that is, the strength of spin-orbit coupling is finite $\alpha_R > 0$, and the Zeeman field is larger than the critical value, $|\vec{E}_{Z,R}| > \sqrt{\Delta_0^2 + \mu_R^2}$. Under these conditions and provided the wire is long enough, there will be an unpaired MZM with a particle-hole-symmetric wave function $[\xi_\uparrow(x), \xi_\downarrow(x), \xi_\uparrow^*(x), \xi_\downarrow^*(x)]^\intercal$ exponentially localized at $x = x_R$. At the same time, we assume that the left lead is subject to a Zeeman field pointing in an arbitrary direction, possibly different from that of $\vec{E}_{Z,R}$, parametrized by angles θ and ϕ (Fig. 1) so that $\vec{E}_{Z,L} = E_{Z,L}(\sin\theta\cos\phi, \sin\theta\sin\phi, \cos\theta)$. We further assume that the left lead has no spin-orbit coupling, $\alpha_L = 0$, and that $E_{Z,L} < \Delta_0$ to guarantee a finite energy gap. Under these conditions, the amplitude of Cooper pair transfer via the MZM is [45]

$$\mathcal{A}^M = \nu_L f\left(\frac{E_{Z,L}}{\Delta_0}\right) [(\xi_\downarrow^2 e^{i\phi} - \xi_\uparrow^2 e^{-i\phi}) \sin\theta + 2\xi_\uparrow\xi_\downarrow \cos\theta], \quad (6)$$

with $f(x) = \frac{\arcsin(x)}{2\sqrt{1-x^2}}$ [46]. Equation (6) is the central result of our work and deserves several comments.

First, if $E_{Z,L} = 0$, $\mathcal{A}^M = 0$, and the Majorana-induced supercurrent is blockaded [35]. Although Eq. (6) assumes no spin-orbit coupling in the trivial SC lead, the blockade of the Majorana-induced supercurrent is more general, and it relies on the presence of TRS in the left lead. In particular, it holds in the presence of spin-orbit coupling as well as nonmagnetic disorder, as we derive in Appendix C [45]. A finite $E_{Z,L}$, however, breaks TRS in the left lead, and according to Eq. (6), a supercurrent can flow via the MZM. The magnitude of $\mathcal{A}^M$ increases linearly for a small Zeeman field, $\mathcal{A}^M \propto E_{Z,L}/\Delta_0$ for $E_{Z,L} \ll \Delta_0$.

Second, the magnitude of the supercurrent also depends crucially on the direction of $\vec{E}_{Z,L}$, a fact which can be understood as follows. On the one hand, because Cooper pairs in the left lead have zero angular momentum, they are composed of two electrons with opposite spin polarizations along the direction dictated by $\vec{E}_{Z,L}$. The two paired electrons must both tunnel through the MZM in order for $\mathcal{A}^M$ to be finite. However, the MZM has its own spin polarization—i.e., the orientation along the Bloch sphere associated with the spinor $[\xi_\uparrow(x_R), \xi_\downarrow(x_R)]^\intercal$—and therefore acts as a spin filter. Thus, if

$\vec{E}_{Z,L}$ is parallel (or antiparallel) to the spin polarization of the Majorana wave function, the supercurrent will vanish.

Third, the amplitude $\mathcal{A}^M$ is, in general, complex, which means that the MZM can contribute to an anomalous supercurrent. Note that the Majorana wave function components ξ_σ are real if the Zeeman field in the right lead has no component along the spin-orbit field direction y [47]. In this case, the phase $\varphi_0^M = \arg(\mathcal{A}^M)$ of the amplitude is controlled only by the direction of $\vec{E}_{Z,L}$.

We can illustrate the previous points with simple limits of Eq. (6). Consider, for instance, the case in which $\vec{E}_{Z,L}$ lies in the xz plane, i.e., $\vec{E}_{Z,L} \cdot \vec{\sigma} = E_Z(\cos\theta\,\sigma_z + \sin\theta\,\sigma_x)$ [$\phi = 0$ in Eq. (6)], while $\vec{E}_{Z,R}$ points along the wire. Then,

$$\mathcal{A}^M = \nu_L f\left(\frac{E_{Z,L}}{\Delta_0}\right)[(\xi_\downarrow^2 - \xi_\uparrow^2)\sin\theta + 2\xi_\uparrow\xi_\downarrow\cos\theta], \qquad (7)$$

with real wave functions ξ_σ. We see that $\mathcal{A}^M$ vanishes if $\theta = \pi/2$ and the MZM is polarized along the x axis ($\xi_\uparrow^2 = \xi_\downarrow^2$) and likewise if $\theta = 0$ and the MZM is spin polarized along the z axis ($\xi_\uparrow\xi_\downarrow = 0$). Furthermore, $\mathcal{A}^M$ is real, and thus, the MZM does not induce any anomalous supercurrent. The fundamental reason for the absence of phase shift ($\varphi_0 = 0$) is that the one-dimensional semiconductor-superconductor nanowire has an additional chiral symmetry (the reality of the Bogoliubov–de Gennes Hamiltonian) when the applied Zeeman field is perpendicular to the Rashba spin-orbit field [47,48]. By contrast, once the Zeeman field has some component along the spin-orbit field σ_y, the chiral symmetry is broken, and the phase shift becomes finite, as indicated by Eq. (6) with $\phi \neq 0$. In particular, when the Zeeman field inside the trivial lead is parallel to the y axis ($\theta = \pi/2$, $\phi = \pi/2$), i.e., $\vec{E}_{Z,L} \cdot \vec{\sigma} = E_{Z,L}\sigma_y$, we have

$$\mathcal{A}^M = i\nu_L f\left(\frac{E_{Z,L}}{\Delta_0}\right)(\xi_\downarrow^2 + \xi_\uparrow^2) \quad \Rightarrow \quad \varphi_0^M = \pi/2. \quad (8)$$

Equations (6), (7), and (8) show that a Zeeman field inside the trivial lead can generate a Majorana-induced supercurrent in a trivial-topological superconductor junction and furthermore that it can lead to anomalous supercurrent. Although we have assumed zero spin-orbit coupling inside the trivial lead to derive a closed form of Eq. (6), such an assumption is not essential, and all the qualitative behavior of $\mathcal{A}^M$ will carry over for finite α_L, as we will show in the following. Note that even though the Majorana-induced supercurrent may be zero, in general, the junction will have a finite supercurrent due to the contribution from the above-gap continuum states in the topological superconductor. We now resort to numerical simulations in order to compute the total critical current; we will also use this opportunity to relax the simplifying assumptions of the analytical calculation.

IV. NUMERICAL SIMULATIONS

To get $I(\varphi)$ numerically, we first calculate the eigenenergies and eigenfunctions for the discretized models of the leads in Eq. (2) using the KWANT package [49] and then plug them into Eqs. (4) and (5). The parameters are chosen to be $m^* = 0.015m_e$, $\alpha_L = \alpha_R = 0.5\,\text{eV\AA}$ ($E_{so} = \frac{1}{2}m^*\alpha^2/\hbar^2 \approx 0.25\,\text{meV}$), $\Delta_0 = 0.4\,\text{meV}$, $\mu_L = 5\,\text{meV}$, and $L = 3.5\,\mu\text{m}$. In
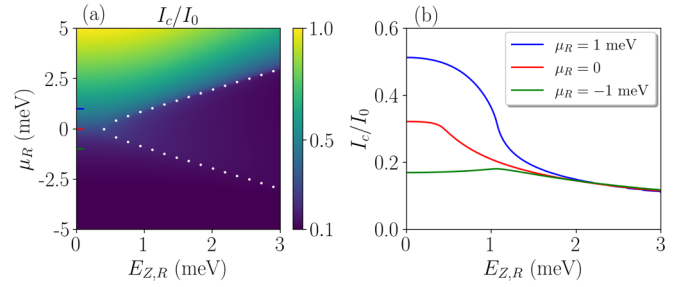

FIG. 2. Critical Josephson current in a junction between a time-reversal-invariant trivial superconductor and a Majorana nanowire lead, with an external Zeeman field $E_{Z,R}\sigma_x$ applied only inside the Majorana nanowire. (a) I_c as a function of $E_{Z,R}$ and μ_R, with white dots representing the phase boundary ($E_{Z,R}^2 = \mu_R^2 + \Delta_0^2$) of the Majorana nanowire. (b) Linecuts of I_c at fixed values of μ_R. Here the supercurrent is due to above-gap continuum states, without any Majorana contribution. When Zeeman field is larger than the critical value ($E_{Z,R} \gtrsim \sqrt{\mu_R^2 + \Delta_0^2}$), I_c plunges with the field strength, indicating the topological quantum phase transition of the Majorana nanowire.

the figures, we adopt the value of critical current at $E_{Z,L} = E_{Z,R} = 0$ and $\mu_R = 5\,\text{meV}$ as a unit of supercurrent I_0.

Figure 2 shows the supercurrent in a junction between a time-reversal-invariant trivial superconducting lead and a Majorana nanowire lead. A Zeeman field along the wire axis is applied only inside the Majorana nanowire lead (i.e., $E_{Z,R}\sigma_x$ and $E_{Z,L} = 0$). All the supercurrent originates from the above-gap contribution to Eq. (5), while the Majorana-induced supercurrent is blockaded due to the TRS in the trivial lead. Figure 2(a) shows the critical current I_c as a function of Zeeman field $E_{Z,R}$ and the chemical potential μ_R of the right lead. In general, the supercurrent is larger when the Majorana nanowire has positive μ_R and is in the topologically trivial phase $E_{Z,R} < \sqrt{\mu_R^2 + \Delta_0^2}$. Figure 2(b) shows linecuts of critical current as a function of Zeeman field at fixed values of chemical potential $\mu_R = 0, \pm 1\,\text{meV}$. The critical current decreases monotonically with the field strength (except for negative μ_R, where the electron density is increased by increasing the Zeeman splitting), and in particular, I_c plunges abruptly near the critical Zeeman field, indicating the topological quantum phase transition of the Majorana nanowire. These results reproduce previous findings of Ref. [38].

In Fig. 3, we show the calculated supercurrent in a junction between a trivial superconductor and a Majorana nanowire lead, with a Zeeman field along the wire axis being applied globally ($E_Z\sigma_x$ in both leads). In contrast to Fig. 2, now the supercurrent in the topological regime ($E_Z > E_{Zc}$) is also large, as shown in Fig. 3(a), because the Majorana-induced supercurrent is finite when TRS in the trivial lead is broken. Figure 3(b) shows several linecuts of I_c as a function of E_Z at fixed values of μ_R (solid lines). Instead of monotonically decreasing, the critical current now increases with the field when the Majorana nanowire enters the topologically nontrivial phase. As shown by the dashed lines in Fig. 3(b), the dominant contribution to I_c deep into the topological phase comes from the MZM, which is consistent with Eq. (7). The oscillations of I_c at large E_Z are due to the onset of a
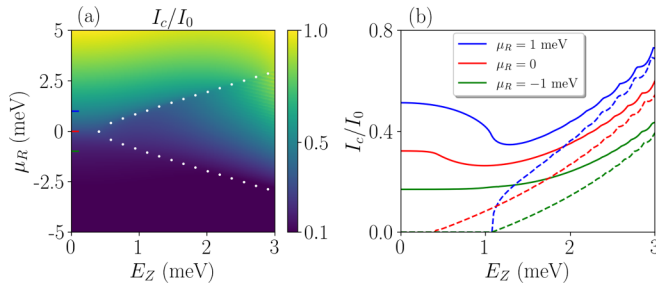
FIG. 3. Critical current in a junction between a trivial superconductor and a Majorana nanowire lead, with an external Zeeman field applied equally in both leads $E_Z\sigma_x$. (a) I_c as a function of E_Z and μ_R, with white dots representing the phase boundary ($E_Z^2 = \mu_R^2 + \Delta_0^2$) of the Majorana nanowire. (b) Linecuts of I_c at fixed values of μ_R. Solid lines are the total critical current from both MZM and continuum states, while dashed lines are critical current due to only MZM.

finite overlap between two MZMs at the opposite ends of the nanowire.

Finally, we consider a Josephson junction for which the Zeeman field is applied globally and has a nonzero component along the spin-orbit field [50,51]. Namely, the Zeeman field takes the form $\vec{E}_Z \cdot \vec{\sigma} = E_Z^x \sigma_x + E_Z^y \sigma_y$ in both leads, with the σ_y component being fixed at $E_Z^y = 0.2\,\mathrm{meV} < \Delta_0$. Here the $E_Z^y \sigma_y$ term breaks the chiral symmetry of the junction leads and thereby can induce anomalous supercurrent. Figure 4 shows the corresponding anomalous supercurrent $I_{an} = I_c \sin(\varphi_0)$ and phase shift φ_0 in the junction. As shown in Figs. 4(a) and 4(c), I_{an} and φ_0 are noticeably large inside the topologically nontrivial regime $[(E_Z^x)^2 + (E_Z^y)^2 > \mu_R^2 + \Delta_0^2]$ due to the Majorana contribution. Figures 4(b) and 4(d) show linecuts of I_{an} and φ_0 at fixed μ_R. For zero and negative μ_R (red and green curves), I_{an} and φ_0 become finite only when the Majorana nanowire enters the topological phase because the continuum state induced supercurrent is negligible. In contrast, for positive μ_R (blue curves), I_{an} and φ_0 do not vanish in the topologically trivial regime owing to finite contributions from the continuum states. However, a kink in I_{an} or an abrupt increase of φ_0 shows up near the critical Zeeman field, signaling the topological quantum phase transition.

V. DISCUSSION

We have studied the Josephson current in a nanowire junction between trivial and topological superconductors. We find that a finite Zeeman field in the trivial lead can switch on the Majorana-induced supercurrent and enhance the critical supercurrent. Furthermore, if the Zeeman field has a component along the spin-orbit field, a MZM can be signaled by the anomalous supercurrent or phase shift. Therefore, a measurement of the dc Josephson current in a trivial-topological superconductor junction as a function of magnetic field and chemical potential could provide compelling evidence for MZMs. In this respect, our findings parallel those previously obtained for junctions of two topological superconductors [52–60]. However, the current proposal simplifies considerably the tuning process of the device by requiring only one superconductor lead to be in the topological phase. In particular, our proposal provides a way for tuning up Majorana
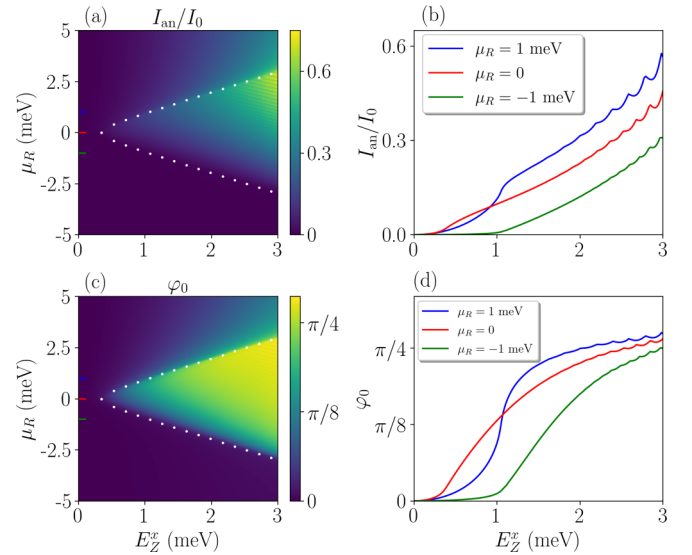

FIG. 4. Anomalous supercurrent I_{an} and phase shift φ_0 for the Josephson junction with a Zeeman field applied globally in the form of $\vec{E}_Z \cdot \vec{\sigma} = E_Z^x \sigma_x + E_Z^y \sigma_y$. The component along the spin-orbit field is fixed at $E_Z^y = 0.2\,\mathrm{meV}$. (a) and (c) I_{an} and φ_0 as a function of μ_R and E_Z^x. Their values in the topological regime are much larger than in the trivial regime due to the Majorana contribution. Here white dots represent the phase boundary $(E_Z^x)^2 + (E_Z^y)^2 = \mu_R^2 + \Delta_0^2$. (b) and (d) Linecuts of I_{an} and φ_0 for fixed values of μ_R. Note that I_{an} and φ_0 increase abruptly near the topological transition.

superconducting qubit devices [30] without the need to add additional probes to their proposed design.

Finally, a few limitations in our work need to be mentioned. For example, although the Majorana signatures proposed in this work are robust against weak nonmagnetic disorders, it may be hard to distinguish Majoranas from smooth-potential-induced low-energy Andreev bound states or quasi-Majoranas within this proposal [61–67] because the supercurrent is induced only by local tunneling processes. Also, the orbital effect of magnetic field and multisubband effects are not discussed, which requires a model study for two- or three-dimensional systems [68–71]. Finally, the point contact model for the tunneling junction may be too simple to describe the coupling between the two segments of the wire. We thus expect that this work will motivate more investigations on similar Josephson junction devices at a more realistic level.

The data set and code for generating the figures in this work can be found in Ref. [72].

ACKNOWLEDGMENTS

APPENDIX A: DERIVATION OF THE GENERAL FORMULA FOR SUPERCURRENT

We derive the formula for the supercurrent through the Josephson junction in the tunneling limit, as shown in Eqs. (4) and (5). The electron operators in the tunneling Hamiltonian H_{tunn} can be expanded in terms of Bogoliubov quasiparticle operators in the corresponding superconducting lead as

$$c_{j\sigma}(x) = \sum_n u_{jn\sigma}(x)\Gamma_{jn} + v_{jn\sigma}^*(x)\Gamma_{jn}^\dagger, \tag{A1}$$

where $j = L/R$, $\Gamma_{jn}^\dagger$ creates a Bogoliubov quasiparticle with excitation energy E_{jn} in lead j, and $[u_{jn\uparrow}(x), u_{jn\downarrow}(x), v_{jn\uparrow}(x), v_{jn\downarrow}(x)]^\mathsf{T}$ is the corresponding Nambu wave function. Using the perturbation theory, the phase-dependent part of the ground-state energy is

$$
\begin{aligned}
E_{gs}(\varphi) &= -\langle\Omega_0|H_{\text{tunnel}}H_0^{-1}H_{\text{tunnel}}|\Omega_0\rangle \\
&= -t^2 e^{i\varphi} \sum_{\sigma,\eta=\uparrow\downarrow} \langle\Omega_0|[c_{R\sigma}^\dagger(x_R)c_{L\sigma}(x_L)]H_0^{-1}[c_{R\sigma}^\dagger(x_R)c_{L\sigma}(x_L)]|\Omega_0\rangle + \text{H.c.} \\
&= -t^2 e^{i\varphi} \sum_{\sigma,\eta=\uparrow\downarrow} \sum_{n,m} \langle\Omega_0|[v_{Rm\eta}(x_R)\Gamma_{Rm}u_{Ln\eta}(x_L)\Gamma_{Ln}]H_0^{-1}[u_{Rm\sigma}^*(x_R)\Gamma_{Rm}^\dagger v_{Ln\sigma}^*(x_L)\Gamma_{Ln}^\dagger]|\Omega_0\rangle + \text{H.c.} \\
&= t^2 e^{i\varphi} \sum_{\sigma,\eta=\uparrow\downarrow} \sum_{n,m} \frac{u_{Ln\eta}(x_L)v_{Ln\sigma}^*(x_L)v_{Rm\eta}(x_R)u_{Rm\sigma}^*(x_R)}{E_{Ln}+E_{Rm}} + \text{H.c.}
\end{aligned} \tag{A2}
$$

If we further define the Cooper pair transfer amplitude $\mathcal{A}$ as

$$\mathcal{A} = \sum_{\eta,\sigma=\uparrow\downarrow} \sum_{n,m} \frac{u_{Ln\eta}(x_L)v_{Ln\sigma}^*(x_L)v_{Rm\eta}(x_R)u_{Rm\sigma}^*(x_R)}{E_{Ln}+E_{Rm}}, \tag{A3}$$

the ground-state energy becomes

$$E_{gs}(\varphi) = t^2(e^{i\varphi}\mathcal{A} + e^{-i\varphi}\mathcal{A}^*) = 2t^2|\mathcal{A}|\cos(\varphi+\varphi_0), \tag{A4}$$

where $\varphi_0 = \arg(\mathcal{A})$. Therefore, the current-phase relation is

$$I(\varphi) = -\frac{2e}{\hbar}\frac{\partial E_{gs}(\varphi)}{\partial\varphi} = \frac{4et^2}{\hbar}|\mathcal{A}|\sin(\varphi+\varphi_0) = I_c\sin(\varphi+\varphi_0), \tag{A5}$$

where $I_c = 4et^2|\mathcal{A}|/\hbar$.

APPENDIX B: TRANSFER AMPLITUDE FOR FINITE ZEEMAN FIELD INSIDE THE TRIVIAL LEAD

The Hamiltonian for the Josephson junction we consider is

$$
\begin{aligned}
H_L &= \sum_{\sigma=\uparrow\downarrow} \int dx\, c_{L\sigma}^\dagger \left(\frac{-\partial_x^2}{2m^*} - \mu_L + \vec{E}_{Z,L}\cdot\vec{\sigma}\right)_{\sigma\sigma'} c_{L\sigma'} + \Delta_0 \int dx(c_{L\downarrow}c_{L\uparrow} + c_{L\uparrow}^\dagger c_{L\downarrow}^\dagger) \\
&= \sum_{\sigma,\sigma'=+/-} \int dx\, c_{L\sigma}^\dagger \left(\frac{-\partial_x^2}{2m^*} - \mu_L + E_{Z,L}\tilde{\sigma}_z\right)_{\sigma\sigma'} c_{L\sigma'} + \Delta_0 \int dx(c_{L-}c_{L+} + c_{L+}^\dagger c_{L-}^\dagger),
\end{aligned}
$$
$$
H_{\text{tunn}} = -te^{i\varphi/2} \sum_{\sigma=+/-} c_{R\sigma}^\dagger(x_R)c_{L\sigma}(x_L) + \text{H.c.} \tag{B1}
$$

Here we rotate the spin basis from $|\uparrow\rangle, |\downarrow\rangle$ to $|+\rangle, |-\rangle$, where $|+\rangle, |-\rangle$ are the eigenstates of $\vec{E}_{Z,L}\cdot\vec{\sigma}$. Thus, the Zeeman term becomes diagonal in the rotated basis, i.e., $\vec{E}_{Z,L}\cdot\vec{\sigma} \to E_{Z,L}\tilde{\sigma}_z$. On the other hand, the electron operators can be expanded as

$$c_{L+}(x_L) = \sum_k (\tilde{u}_n\Gamma_{n,+} - \tilde{v}_n\Gamma_{\bar{n},-}^\dagger),$$

$$c_{L-}(x_L) = \sum_k (\tilde{u}_n\Gamma_{\bar{n},-} + \tilde{v}_n\Gamma_{n,+}^\dagger), \quad c_{R\sigma}(x_R) = \xi_\sigma(x_R)\gamma, \tag{B2}$$

where $\Gamma_{n,+}^\dagger$ and $\Gamma_{\bar{n},-}^\dagger$ create the Bogoliubov quasiparticles of excitation energy $E_{n\pm} = \sqrt{\varepsilon_n^2 + \Delta_0^2} \pm E_{Z,L}$, with $\varepsilon_n = \xi_n - \mu_L$. $\tilde{u}_n, \tilde{v}_n$ are BCS coherence factors with $\tilde{u}_n^2 = \frac{1}{2} + \frac{\varepsilon_n}{2\sqrt{\varepsilon_n^2 + \Delta_0^2}} = 1 - \tilde{v}_n^2$. Substituting them into Eq. (4), we get

$$
\begin{aligned}
\mathcal{A}^M &= \xi_+(x_R)\xi_-(x_R) \sum_n \tilde{u}_n \tilde{v}_n \left(\frac{1}{\sqrt{\varepsilon_n^2 + \Delta_0^2} - E_{Z,L}} - \frac{1}{\sqrt{\varepsilon_n^2 + \Delta_0^2} + E_{Z,L}} \right) \\
&= \xi_+(x_R)\xi_-(x_R) \nu_L \int d\varepsilon_n \frac{\Delta_0 E_{Z,L}}{\sqrt{\varepsilon_n^2 + \Delta_0^2}(\varepsilon_n^2 + \Delta_0^2 - E_{Z,L}^2)} \\
&= \nu_L \xi_+(x_R)\xi_-(x_R) \frac{\arcsin(E_{Z,L}/\Delta_0)}{\sqrt{\Delta_0^2 - E_{Z,L}^2}}
\end{aligned}
\tag{B3}
$$

for $E_{Z,L} < \Delta_0$. Finally, we rotate the spin basis back to $|\uparrow\rangle, |\downarrow\rangle$ along the spin-z direction by the following unitary transformation

$$
\begin{pmatrix} \xi_+ \\ \xi_- \end{pmatrix} = \begin{pmatrix} \cos(\theta/2)e^{-i\phi} & \sin(\theta/2) \\ -\sin(\theta/2) & \cos(\theta/2)e^{i\phi} \end{pmatrix} \begin{pmatrix} \xi_\uparrow \\ \xi_\downarrow \end{pmatrix},
\tag{B4}
$$

such that the transfer amplitude becomes

$$
\mathcal{A}^M = \nu_L \frac{\arcsin(E_{Z,L}/\Delta_0)}{2\sqrt{\Delta_0^2 - E_{Z,L}^2}} [(\xi_\downarrow^2 e^{i\phi} - \xi_\uparrow^2 e^{-i\phi})\sin\theta + 2\xi_\uparrow \xi_\downarrow \cos\theta].
\tag{B5}
$$

APPENDIX C: MAJORANA SUPERCURRENT BLOCKADE

The Hamiltonian of a time-reversal-invariant superconductor with s-wave pairing symmetry can always be written in the following form:

$$
H = H_0 + H_{sc} = \sum_n \{\varepsilon_n(a_n^\dagger a_n + a_{\bar{n}}^\dagger a_{\bar{n}}) + \Delta_0(a_{\bar{n}}a_n + a_n^\dagger a_{\bar{n}}^\dagger)\},
\tag{C1}
$$

where a_n is the annihilation operator for a normal eigenstate of eigenenergy ε_n and eigenfunction $\psi_n(x)$. $a_{\bar{n}}$ is the annihilation operator for its time-reversed state which has an eigenenergy $\varepsilon_{\bar{n}} = \varepsilon_n$ and eigenfunction $\psi_{\bar{n}}(x)$. The relation between the original real-space electron operator $c(x)$ and the eigenstate operator a_n is

$$
c_\sigma(x) = \sum_n [\psi_{n\sigma}(x)a_n + \psi_{\bar{n}\sigma}(x)a_{\bar{n}}].
\tag{C2}
$$

On the other hand, since the Hamiltonian in Eq. (C1) is in the BCS form, we can expand the normal operators a_n in terms of the Bogoliubov quasiparticle operators as

$$
\begin{aligned}
a_n &= \tilde{u}_n \Gamma_n - \tilde{v}_n \Gamma_{\bar{n}}^\dagger, \\
a_{\bar{n}} &= \tilde{u}_n \Gamma_{\bar{n}} + \tilde{v}_n \Gamma_n^\dagger,
\end{aligned}
\tag{C3}
$$

where $\Gamma_n^\dagger$ and $\Gamma_{\bar{n}}^\dagger$ create Bogoliubov quasiparticles with excitation energy $E_{\bar{n}} = E_n = \sqrt{\varepsilon_n^2 + \Delta_0^2}$ and $\tilde{u}_n, \tilde{v}_n$ are BCS coherence factors with $\tilde{u}_n^2 = 1/2 + \varepsilon_n/2E_n = 1 - \tilde{v}_n^2$. Substituting Eq. (C3) into Eq. (C2), we get

$$
c_\sigma(x) = \sum_n \{\tilde{u}_n[\psi_{n\sigma}(x)\Gamma_n + \psi_{\bar{n}\sigma}(x)\Gamma_{\bar{n}}] + \tilde{v}_n[\psi_{\bar{n}\sigma}(x)\Gamma_n^\dagger - \psi_{n\sigma}(x)\Gamma_{\bar{n}}^\dagger]\}.
\tag{C4}
$$

After plugging Eq. (C4) into Eq. (5), we have

$$
\begin{aligned}
\mathcal{A}^M &= \sum_{\eta,\sigma=\uparrow\downarrow} \xi_\eta(x_R)\xi_\sigma(x_R) \sum_n \tilde{u}_n \tilde{v}_n \left[\frac{\psi_{n\eta}(x_L)\psi_{\bar{n}\sigma}(x_L)}{E_n} - \frac{\psi_{\bar{n}\eta}(x_L)\psi_{n\sigma}(x_L)}{E_{\bar{n}}} \right] \\
&= \sum_{\eta,\sigma=\uparrow\downarrow} \xi_\eta(x_R)\xi_\sigma(x_R) \sum_n \frac{\tilde{u}_n \tilde{v}_n}{E_n} [\psi_{n\eta}(x_L)\psi_{\bar{n}\sigma}(x_L) - \psi_{n\sigma}(x_L)\psi_{\bar{n}\eta}(x_L)] \\
&= \sum_{\eta,\sigma=\uparrow\downarrow} \mathcal{A}_{\eta\sigma}^M.
\end{aligned}
\tag{C5}
$$

For $\eta = \sigma$,

$$\mathcal{A}_{\sigma\sigma}^M \propto [\psi_{n\sigma}(x_L)\psi_{\bar{n}\sigma}(x_L) - \psi_{n\sigma}(x_L)\psi_{\bar{n}\sigma}(x_L)] = 0. \tag{C6}$$

For $\eta \neq \sigma$,

$$\mathcal{A}_{\downarrow\uparrow}^M + \mathcal{A}_{\uparrow\downarrow}^M \propto [\psi_{n\downarrow}(x_L)\psi_{\bar{n}\uparrow}(x_L) - \psi_{n\uparrow}(x_L)\psi_{\bar{n}\downarrow}(x_L)] + [\psi_{n\uparrow}(x_L)\psi_{\bar{n}\downarrow}(x_L) - \psi_{n\downarrow}(x_L)\psi_{\bar{n}\uparrow}(x_L)] = 0. \tag{C7}$$

Therefore, Majorana-induced supercurrent is completely blockaded when the trivial superconducting lead is time reversal invariant.

[1] J. Alicea, New directions in the pursuit of Majorana fermions in solid state systems, Rep. Prog. Phys. **75**, 076501 (2012).

[2] M. Leijnse and K. Flensberg, Introduction to topological superconductivity and Majorana fermions, Semicond. Sci. Technol. **27**, 124003 (2012).

[3] C. W. J. Beenakker, Search for Majorana fermions in superconductors, Annu. Rev. Condens. Matter Phys. **4**, 113 (2013).

[4] T. D. Stanescu and S. Tewari, Majorana fermions in semiconductor nanowires: Fundamentals, modeling, and experiment, J. Phys.: Condens. Matter **25**, 233201 (2013).

[5] J.-H. Jiang and S. Wu, Non-Abelian topological superconductors from topological semimetals and related systems under the superconducting proximity effect, J. Phys.: Condens. Matter **25**, 055701 (2013).

[6] S. R. Elliott and M. Franz, Colloquium: Majorana fermions in nuclear, particle, and solid-state physics, Rev. Mod. Phys. **87**, 137 (2015).

[7] M. Sato and S. Fujimoto, Majorana fermions and topology in superconductors, J. Phys. Soc. Jpn. **85**, 072001 (2016).

[8] M. Sato and Y. Ando, Topological superconductors: A review, Rep. Prog. Phys. **80**, 076501 (2017).

[9] R. Aguado, Majorana quasiparticles in condensed matter, Riv. Nuovo Cimento Soc. Ital. Fis. **40**, 523 (2017).

[10] R. M. Lutchyn, E. P. A. M. Bakkers, L. P. Kouwenhoven, P. Krogstrup, C. M. Marcus, and Y. Oreg, Majorana zero modes in superconductor–semiconductor heterostructures, Nat. Rev. Mater. **3**, 52 (2018).

[11] H. Zhang, D. E. Liu, M. Wimmer, and L. P. Kouwenhoven, Next steps of quantum transport in Majorana nanowire devices, Nat. Commun. **10**, 5128 (2019).

[12] S. M. Frolov, M. J. Manfra, and J. D. Sau, Topological superconductivity in hybrid devices, Nat. Phys. **16**, 718 (2020).

[13] C. Nayak, S. H. Simon, A. Stern, M. Freedman, and S. Das Sarma, Non-Abelian anyons and topological quantum computation, Rev. Mod. Phys. **80**, 1083 (2008).

[14] S. D. Sarma, M. Freedman, and C. Nayak, Majorana zero modes and topological quantum computation, npj Quantum Inf. **1**, 15001 (2015).

[15] J. D. Sau, R. M. Lutchyn, S. Tewari, and S. Das Sarma, Generic New Platform for Topological Quantum Computation Using Semiconductor Heterostructures, Phys. Rev. Lett. **104**, 040502 (2010).

[16] R. M. Lutchyn, J. D. Sau, and S. Das Sarma, Majorana Fermions and a Topological Phase Transition in Semiconductor-Superconductor Heterostructures, Phys. Rev. Lett. **105**, 077001 (2010).

[17] Y. Oreg, G. Refael, and F. von Oppen, Helical Liquids and Majorana Bound States in Quantum Wires, Phys. Rev. Lett. **105**, 177002 (2010).

[18] J. D. Sau, S. Tewari, R. M. Lutchyn, T. D. Stanescu, and S. Das Sarma, Non-Abelian Quantum Order in Spin-Orbit-Coupled Semiconductors: Search for Topological Majorana Particles in Solid-State Systems, Phys. Rev. B **82**, 214509 (2010).

[19] V. Mourik, K. Zuo, S. M. Frolov, S. R. Plissard, E. P. A. M. Bakkers, and L. P. Kouwenhoven, Signatures of Majorana fermions in hybrid superconductor-semiconductor nanowire devices, Science **336**, 1003 (2012).

[20] A. Das, Y. Ronen, Y. Most, Y. Oreg, M. Heiblum, and H. Shtrikman, Zero-bias peaks and splitting in an Al-InAs nanowire topological superconductor as a signature of Majorana fermions, Nat. Phys. **8**, 887 (2012).

[21] M. T. Deng, C. L. Yu, G. Y. Huang, M. Larsson, P. Caroff, and H. Q. Xu, Anomalous zero-bias conductance peak in a Nb-InSb nanowire-Nb hybrid device, Nano Lett. **12**, 6414 (2012).

[22] H. O. H. Churchill, V. Fatemi, K. Grove-Rasmussen, M. T. Deng, P. Caroff, H. Q. Xu, and C. M. Marcus, Superconductor-nanowire devices from tunneling to the multichannel regime: Zero-bias oscillations and magnetoconductance crossover, Phys. Rev. B **87**, 241401(R) (2013).

[23] A. D. K. Finck, D. J. Van Harlingen, P. K. Mohseni, K. Jung, and X. Li, Anomalous Modulation of a Zero-Bias Peak in a Hybrid Nanowire-Superconductor Device, Phys. Rev. Lett. **110**, 126406 (2013).

[24] S. M. Albrecht, A. P. Higginbotham, M. Madsen, F. Kuemmeth, T. S. Jespersen, J. Nygård, P. Krogstrup, and C. M. Marcus, Exponential protection of zero modes in Majorana islands, Nature (London) **531**, 206 (2016).

[25] J. Chen, P. Yu, J. Stenger, M. Hocevar, D. Car, S. R. Plissard, E. P. A. M. Bakkers, T. D. Stanescu, and S. M. Frolov, Experimental phase diagram of zero-bias conductance peaks in superconductor/semiconductor nanowire devices, Sci. Adv. **3**, e1701476 (2017).

[26] M. T. Deng, S. Vaitiekenas, E. B. Hansen, J. Danon, M. Leijnse, K. Flensberg, J. Nygård, P. Krogstrup, and C. M. Marcus, Majorana bound state in a coupled quantum-dot hybrid-nanowire system, Science **354**, 1557 (2016).

[27] H. Zhang *et al.*, Ballistic superconductivity in semiconductor nanowires, Nat. Commun. **8**, 16025 (2017).

[28] Ö. Gül, H. Zhang, J. D. S. Bommer, M. W. A. de Moor, D. Car, S. R. Plissard, E. P. A. M. Bakkers, A. Geresdi, K. Watanabe, T. Taniguchi, and L. P. Kouwenhoven, Ballistic Majorana nanowire devices, Nat. Nanotechnol. **13**, 192 (2018).

[29] F. Nichele, A. C. C. Drachmann, A. M. Whiticar, E. C. T. O'Farrell, H. J. Suominen, A. Fornieri, T. Wang, G. C. Gardner, C. Thomas, A. T. Hatke, P. Krogstrup, M. J. Manfra, K. Flensberg, and C. M. Marcus, Scaling of Majorana Zero-Bias Conductance Peaks, Phys. Rev. Lett. **119**, 136803 (2017).

[30] C. Schrade and L. Fu, Majorana Superconducting Qubit, Phys. Rev. Lett. **121**, 267002 (2018).

[31] Y. Peng, F. Pientka, Y. Vinkler-Aviv, L. I. Glazman, and F. von Oppen, Robust Majorana Conductance Peaks for a Superconducting Lead, Phys. Rev. Lett. **115**, 266804 (2015).

[32] D. Chevallier and J. Klinovaja, Tomography of Majorana fermions with STM tips, Phys. Rev. B **94**, 035417 (2016).

[33] F. Setiawan, W. S. Cole, J. D. Sau, and S. Das Sarma, Conductance spectroscopy of nontopological-topological superconductor junctions, Phys. Rev. B **95**, 020501(R) (2017).

[34] F. Setiawan, W. S. Cole, J. D. Sau, and S. Das Sarma, Transport in superconductor–normal metal–superconductor tunneling structures: Spinful p-wave and spin-orbit-coupled topological wires, Phys. Rev. B **95**, 174515 (2017).

[35] A. Zazunov and R. Egger, Supercurrent blockade in Josephson junctions with a Majorana wire, Phys. Rev. B **85**, 104514 (2012).

[36] P. A. Ioselevich, P. M. Ostrovsky, and M. V. Feigel'man, Josephson current between topological and conventional superconductors, Phys. Rev. B **93**, 125435 (2016).

[37] A. Zazunov, R. Egger, and A. Levy Yeyati, Low-energy theory of transport in Majorana wire junctions, Phys. Rev. B **94**, 014502 (2016).

[38] A. Zazunov, A. Iks, M. Alvarado, A. L. Yeyati, and R. Egger, Josephson effect in junctions of conventional and topological superconductors, Beilstein J. Nanotechnol. **9**, 1659 (2018).

[39] A. Schuray, A. L. Yeyati, and P. Recher, Influence of the Majorana nonlocality on the supercurrent, Phys. Rev. B **98**, 235301 (2018).

[40] J. Cayao and A. M. Black-Schaffer, Finite length effect on supercurrents between trivial and topological superconductors, Eur. Phys. J.: Spec. Top. **227**, 1387 (2018).

[41] C. Schrade and L. Fu, Andreev or Majorana, Cooper finds out, arXiv:1809.06370.

[42] C.-H. Lin, J. D. Sau, and S. Das Sarma, Zero-bias conductance peak in Majorana wires made of semiconductor/superconductor hybrid structures, Phys. Rev. B **86**, 224511 (2012).

[43] C.-X. Liu, J. D. Sau, and S. Das Sarma, Role of dissipation in realistic Majorana nanowires, Phys. Rev. B **95**, 054502 (2017).

[44] V. Ambegaokar and A. Baratoff, Tunneling Between Superconductors, Phys. Rev. Lett. **10**, 486 (1963).

[45] See the Appendixes for the details of the derivation of the general formula of the current-phase relation, the amplitude of the Cooper pair transfer via MZM, and the supercurrent blockade.

[46] Note that the divergence of $f(x)$ for $x \rightarrow 1$ is not physical and indicates the breakdown of perturbation theory as the gap closes in the left lead.

[47] S. Tewari and J. D. Sau, Topological Invariants for Spin-Orbit Coupled Superconductor Nanowires, Phys. Rev. Lett. **109**, 150408 (2012).

[48] A. Rasmussen, J. Danon, H. Suominen, F. Nichele, M. Kjaergaard, and K. Flensberg, Effects of spin-orbit coupling and spatial symmetries on the Josephson current in SNS junctions, Phys. Rev. B **93**, 155406 (2016).

[49] C. W. Groth, M. Wimmer, A. R. Akhmerov, and X. Waintal, Kwant: A software package for quantum transport, New J. Phys. **16**, 063065 (2014).

[50] J. D. S. Bommer, H. Zhang, Ö. Gül, B. Nijholt, M. Wimmer, F. N. Rybakov, J. Garaud, D. Rodic, E. Babaev, M. Troyer, D. Car, S. R. Plissard, E. P. A. M. Bakkers, K. Watanabe, T. Taniguchi, and L. P. Kouwenhoven, Spin-orbit Protection of Induced Superconductivity in Majorana Nanowires, Phys. Rev. Lett. **122**, 187702 (2019).

[51] C.-X. Liu, J. D. Sau, T. D. Stanescu, and S. Das Sarma, Conductance smearing and anisotropic suppression of induced superconductivity in a Majorana nanowire, Phys. Rev. B **99**, 024510 (2019).

[52] L. Jiang, D. Pekker, J. Alicea, G. Refael, Y. Oreg, and F. von Oppen, Unconventional Josephson Signatures of Majorana Bound States, Phys. Rev. Lett. **107**, 236401 (2011).

[53] D. M. Badiane, M. Houzet, and J. S. Meyer, Nonequilibrium Josephson Effect Through Helical Edge States, Phys. Rev. Lett. **107**, 177002 (2011).

[54] P. San-Jose, E. Prada, and R. Aguado, ac Josephson Effect in Finite-Length Nanowire Junctions with Majorana Modes, Phys. Rev. Lett. **108**, 257001 (2012).

[55] D. I. Pikulin and Y. V. Nazarov, Phenomenology and dynamics of a Majorana Josephson junction, Phys. Rev. B **86**, 140504(R) (2012).

[56] P. San-Jose, E. Prada, and R. Aguado, Mapping the Topological Phase Diagram of Multiband Semiconductors with Supercurrents, Phys. Rev. Lett. **112**, 137001 (2014).

[57] K. N. Nesterov, M. Houzet, and J. S. Meyer, Anomalous Josephson Effect in Semiconducting Nanowires as a Signature of the Topologically Nontrivial Phase, Phys. Rev. B **93**, 174502 (2016).

[58] P. Marra, R. Citro, and A. Braggio, Signatures of topological phase transitions in Josephson current-phase discontinuities, Phys. Rev. B **93**, 220507(R) (2016).

[59] J. Cayao, P. San-Jose, A. M. Black-Schaffer, R. Aguado, and E. Prada, Majorana splitting from critical currents in Josephson junctions, Phys. Rev. B **96**, 205425 (2017).

[60] C. M. Murthy, V. D. Kurilovich, P. D. Kurilovich, B. van Heck, L. I. Glazman, and C. Nayak, Energy spectrum and current-phase relation of a nanowire Josephson junction close to the topological transition, Phys. Rev. B **101**, 224501 (2020).

[61] G. Kells, D. Meidan, and P. W. Brouwer, Near-zero-energy end states in topologically trivial spin-orbit coupled superconducting nanowires with a smooth confinement, Phys. Rev. B **86**, 100503(R) (2012).

[62] E. Prada, P. San-Jose, and R. Aguado, Transport spectroscopy of NS nanowire junctions with Majorana fermions, Phys. Rev. B **86**, 180503(R) (2012).

[63] C.-X. Liu, J. D. Sau, T. D. Stanescu, and S. Das Sarma, Andreev bound states versus Majorana bound states in quantum dot-nanowire-superconductor hybrid structures: Trivial versus topological zero-bias conductance peaks, Phys. Rev. B **96**, 075161 (2017).

[64] C.-X. Liu, J. D. Sau, and S. Das Sarma, Distinguishing topological Majorana bound states from trivial Andreev bound states: Proposed tests through differential tunneling conductance spectroscopy, Phys. Rev. B **97**, 214502 (2018).

[65] C. Moore, T. D. Stanescu, and S. Tewari, Two-terminal charge tunneling: Disentangling Majorana zero modes from

partially separated Andreev bound states in semiconductor-superconductor heterostructures, Phys. Rev. B **97**, 165302 (2018).

[66] C. Reeg, O. Dmytruk, D. Chevallier, D. Loss, and J. Klinovaja, Zero-energy Andreev bound states from quantum dots in proximitized Rashba nanowires, Phys. Rev. B **98**, 245407 (2018).

[67] A. Vuik, B. Nijholt, A. R. Akhmerov, and M. Wimmer, Reproducing topological properties with quasi-Majorana states, SciPost Phys. **7**, 61 (2019).

[68] R. M. Lutchyn, T. D. Stanescu, and S. Das Sarma, Search for Majorana Fermions in Multiband Semiconducting Nanowires, Phys. Rev. Lett. **106**, 127001 (2011).

[69] B. Nijholt and A. R. Akhmerov, Orbital effect of magnetic field on the Majorana phase diagram, Phys. Rev. B **93**, 235434 (2016).

[70] O. Dmytruk and J. Klinovaja, Suppression of the overlap between Majorana fermions by orbital magnetic effects in semiconducting-superconducting nanowires, Phys. Rev. B **97**, 155409 (2018).

[71] G. W. Winkler, A. E. Antipov, B. van Heck, A. A. Soluyanov, L. I. Glazman, M. Wimmer, and R. M. Lutchyn, Unified numerical approach to topological semiconductor-superconductor heterostructures, Phys. Rev. B **99**, 245408 (2019).

[72] C.-X. Liu, B. van Heck, and M. Wimmer, Josephson current via an isolated Majorana zero mode (2020), doi: 10.5281/zenodo.4291049.